

Stability of Regional Traffic Networks Employing Maximum Throughput Demand Management[★]

Michalis Ramp^{a,*}, Andreas Kasis^a, Charalambos Menelaou^a, Stelios Timotheou^{a,b}

^aKIOS Research and Innovation Center of Excellence, University of Cyprus, 1 Panepistimiou Avenue, 2109, Aglantzia, Nicosia, Cyprus

^bDepartment of Electrical and Computer Engineering, University of Cyprus, 1 Panepistimiou Avenue, 2109, Aglantzia, P.O. Box 20537, CY-1678, Nicosia, Cyprus

Abstract

This paper considers the stability and optimality properties of traffic demand management schemes, motivated by the integration of smart monitoring and control technologies in traffic networks. First, a suitable optimization problem is formulated that aims to obtain demand input values that maximize the throughput within traffic networks adhering to regional traffic dynamics with triangular macroscopic fundamental diagrams. We show that optimal solutions to this problem may lead to unstable behaviour, revealing a trade-off between stability and optimality. To address this issue, we analytically study the stability properties of traffic networks at the presence of constant demand input and provide suitable local conditions that guarantee stability when the system's equilibrium densities are strictly within the free-flow region, but not at the critical density. The latter case is significant, since the maximum throughput behaviour coincides in many cases with the local critical density. We resolve this by proposing a decentralized proportional demand control scheme and suitable local design conditions such that stability is guaranteed. Our analytic results are validated with numerical simulations in a 3-region system that demonstrate the effectiveness and practicality of the proposed approach.

Keywords: Traffic control, Demand management, Large-scale systems, Decentralized control

1. Introduction

Recent technological achievements enabled the evolution of traffic networks to smart networks. This was possible through the incorporation of real-time smart monitoring technologies (connected vehicles, drones, etc.) and the integration of fast communication protocols that enabled the design and application of novel traffic control schemes.

Despite these advancements, urban road networks frequently grapple with inherent congestion issues. This often results due to demand surpassing the available capacity in specific regions, giving rise to undesirable traffic conditions such as congestion [1]. To proactively address these challenges, a plethora of traffic management strategies [2], based on macroscopic traffic dynamics, have been proposed in existing research literature [3].

One such strategy is route guidance (RG) [4], which aims to redistribute vehicular loads across the network. By directing drivers along alternative pathways, this approach aims to

optimize overall travel times [4]. Concurrently, perimeter control (PC) and gating strategies (GS) [5, 6] focus on preemptively mitigating congestion. These methods regulate the inflow of vehicles at the outskirts of a designated, congestion-prone region. By doing so, the core area of this region is able to operate under congestion-free conditions, even though the congestion may subsequently be transferred to the periphery of the urban network [7]. A substantial number of macroscopic strategies rely on Model Predictive Control (MPC) frameworks [8, 9, 10, 11, 12, 13, 14, 15]. Despite their efficacy in handling traffic congestion, MPC methods have limitations. One notable drawback is their tendency to overlook stability issues, which may lead to unpredictable and suboptimal system performance.

Examples of MPC-based solutions include an optimal 2-region PC scheme [9], a two-level hierarchical PC scheme [10], a three-level hierarchical PC scheme [11], a Lyapunov derived PC combined with a distributed MPC [12], a PC nonlinear MPC with stability by construction [13], a joint RG and demand management (DM) MPC [14], and an RG and DM MPC framework proposing two real-time solution approaches [15].

Alternative approaches, aiming to achieve congestion mitigation, include an optimal state-feedback PC strategy for a 2-region network [16], a robust proportional-integral (PI) PC scheme via quantitative feedback [17], a PC strategy employing optimal multivariate PI-feedback generators and online adaptive optimization [18], an RG approach managing congestion at the microscopic level by route reservation in the spatial and temporal domains [19], a model-free data-driven adaptive PC with RG [20] and an approach at the microscopic level propos-

[★]This work is supported by the European Union (i. ERC, URANUS, No. 101088124, and ii. Horizon 2020 Teaming, KIOS CoE, No. 739551), and the Government of the Republic of Cyprus through the Deputy Ministry of Research, Innovation, and Digital Strategy. Views and opinions expressed are however those of the author(s) only and do not necessarily reflect those of the European Union or the European Research Council Executive Agency. Neither the European Union nor the granting authority can be held responsible for them.

^{*}Corresponding author

Email addresses: ramp.michalis@ucy.ac.cy (Michalis Ramp), kasis.andreas@ucy.ac.cy (Andreas Kasis), menelaou.charalampos@ucy.ac.cy (Charalambos Menelaou), timotheou.stelios@ucy.ac.cy (Stelios Timotheou)

ing a joint robust correlated equilibrium routing mechanism and a distributed optimization algorithm for congestion mitigation [21].

Despite the substantial technological advancements and the wide range of traffic management schemes available today, traffic congestion continues to be a pervasive issue [22]. A drawback of several proposed schemes, which may hinder attaining efficient traffic network solutions, is their propensity to prioritize individual needs over achieving a system-wide optimum [23].

Recent works present a promising perspective, advocating for the joint integration of traffic and demand management (DM) strategies as an effective solution to mitigate congestion [14, 15, 19]. Traffic demand management strategies primarily focus on regulating the influx of vehicles into the network. They achieve this by encouraging drivers to opt for alternative travel times, either earlier or later than their initial plans, or to consider different modes of transportation altogether [24]. The joint integration of demand with traffic management enables the redistribution of traffic flows across both temporal and spatial dimensions, aiming to enhance the overall efficiency and performance of the road transportation system [25].

Despite their potential, works that employ DM in a macroscopic framework are limited [14, 15, 19]. The works in [14, 15, 19] rely on MPC approaches and do not consider the DM problem from a stability viewpoint. Considering the stability properties of DM schemes in traffic networks, and how these are affected by optimality considerations, is highly important to enable their large scale implementation.

Contribution: This paper studies the stability and optimality properties of traffic networks at the presence of demand management schemes considering regional traffic dynamics with triangular Macroscopic Fundamental Diagrams (MFDs). Firstly, we formulate a problem that aims to maximize the throughput within a large-scale traffic network and discuss how such problem may be solved using standard optimization tools. However, we show numerically that optimal solutions may lead to unstable behaviour, when those coincide with local critical densities, which is frequently the case. In particular, we demonstrate that under optimal constant demand input, any deviation towards the congested region leads to gridlock behaviour. The latter reveals an inherent trade-off between stability and optimality of DM schemes and motivates the analytical study of the stability properties of such schemes in traffic networks. Our stability analysis provides local conditions on the traffic network parameters that enable stability guarantees, when the local equilibrium densities lie strictly within the free flow region, i.e. being less than the critical density. To include the latter case, which frequently occurs when demand is optimized to maximize throughput, we propose a decentralized proportional feedback demand management scheme and provide local conditions on its gains such that stability is guaranteed. Our analytic results are validated with numerical simulations on a 3-region system which showcase the effectiveness and practicality of the proposed conditions and demand schemes.

The main contributions of this work are summarized below.

- (i) A DM optimization problem that yields throughput-optimal equilibrium behaviour is formulated.
- (ii) A trade-off between optimality and stability in DM schemes in traffic networks is demonstrated, showing that a maximum throughput behaviour may lead to instability.
- (iii) The stability properties of large-scale traffic networks at the presence of constant demand are analytically studied and local conditions such that stability may be deduced are provided. Moreover, a decentralized demand management scheme that offers enhanced stability properties is proposed.

Paper structure: The rest of the paper is organized as follows. In Section 2 the notation used throughout the paper and the traffic network dynamics are provided. Section 3 defines the optimization problem for demand allocation, and presents the problem statement of this work. A discussion on the inherent trade-off between optimality and stability concludes this section. Section 4 presents our main stability results, concerning a constant demand input scheme and a developed decentralized proportional scheme, showcasing the enhanced stability properties of the latter. Section 5 demonstrates the practicality and applicability of the analytic results through simulations on a 3-region network. Conclusions are drawn in Section 6.

2. Problem Formulation

2.1. Notation

Real numbers are denoted by \mathbb{R} , and \mathbb{R}_+ is the set of real non-negative numbers. Vectors are denoted by bold small letters where the i^{th} component of a vector \mathbf{x} is denoted by x_i . The set of n -dimensional vectors with real entries is denoted by \mathbb{R}^n . The non-negative orthant of \mathbb{R}^n is denoted by \mathbb{R}_+^n . Sets are denoted by capital calligraphic letters. The min-max operator is given by $[x]_a^b = \max(\min(x, b), a)$, where $a, b \in \mathbb{R}$ and $a \leq b$. A function $f : \mathbb{R}^n \rightarrow \mathbb{R}$ is positive semidefinite if $f(x) \geq 0$ for all $x \in \mathbb{R}^n$. It is positive definite if $f(0) = 0$ and $f(x) > 0$ for every $x \neq 0$. It is negative definite if $f(0) = 0$ and $f(x) < 0$ for every $x \neq 0$. We write $\mathbf{0} \in \mathbb{R}^n$ to denote the $n \times 1$ vector with all elements equal to 0. A set \mathcal{N} excluding an element i is denoted by $\mathcal{N} \setminus \{i\}$. The hat designation, \hat{x}_i , denotes that x_i is a primal or dual optimal element with respect to a given optimization problem whereas the right superscript x_i^* denotes a system equilibrium. For compactness, we write the units of the considered variables at the first instance only.

2.2. Model description

The behaviour of the traffic area under interest is modelled as a *network* of n homogeneous regions ($n \geq 2$) connected by *edges* between *nodes*. A directed graph $\mathcal{G} = \{\mathcal{N}, \mathcal{E}\}$ captures the network structure where the sets of nodes and edges are denoted by $\mathcal{N} = \{1, 2, \dots, n\}$, and $\mathcal{E} \subseteq \mathcal{N} \times \mathcal{N}$, respectively. Onward the term node and region are used interchangeably. The edge allowing region j to receive vehicles from region i , is denoted by $\epsilon_{i,j} = (i, j) \in \mathcal{E}$. Regions that can directly send vehicles to region i belong to the set $\mathcal{P}_i = \{j \in \mathcal{N} : \epsilon_{j,i} \in \mathcal{E}\}$ and are termed

predecessors, while regions that directly receive vehicles from region i belong to the set $\mathcal{S}_i = \{l \in \mathcal{N} : \epsilon_{i,l} \in \mathcal{E}\}$ and are termed successors. Vehicle inflow to the multi-region traffic network occurs via origin regions. All regions are considered to be both origin and destination regions, where it is assumed that every vehicle that enters the network, does so to reach a destination region that belongs to the network.

The internal traffic flow¹, $q_i(t)$ [veh/h], in any region i of the traffic network, is equal to the product between vehicle density, $\rho_i(t)$ [veh/km], and vehicle speed, $v_i(t)$ [km/h] of the same region, i.e.

$$q_i(t) = \rho_i(t)v_i(t), i \in \mathcal{N}. \quad (1)$$

Also, for the considered traffic network, homogeneity conditions dictate that the behaviour of the internal traffic flow, $q_i(t)$, in any region i is described by a triangular fundamental diagram (FD)

$$q_i(t) = f_i(\rho_i(t)), i \in \mathcal{N}. \quad (2)$$

i.e., a piecewise-linear concave function, $f_i(\rho_i(t))$.

A triangular MFD [3, 26, 27], see Fig. 1, defines the aggregated traffic behaviour of region i by connecting the region i internal flow, $q_i(t)$, with the total inter-regional flow of region i , $g_i(\rho_i(t))$ [veh/h], resulting in homogeneous behaviour.

Two traffic states characterize the total inter-regional flow of region i , $g_i(\rho_i(t))$, see Fig. 1. They are defined by the critical density threshold of region i , ρ_i^C [veh/km], and the jam density threshold of region i , ρ_i^J [veh/km], as

$$g_i(\rho_i) = \begin{cases} r_i f_i(\rho_i) = r_i v_i^f \rho_i, & \rho_i \leq \rho_i^C \\ r_i f_i(\rho_i) = (b_i^C - v_i^C \rho_i) r_i, & \rho_i > \rho_i^C \end{cases}, \quad (3)$$

for all $i \in \mathcal{N}$ and where, $r_i \in \mathbb{R}_+$ is the region i trip completion ratio given by

$$r_i = L_i l_i^{-1}, \quad (4)$$

where L_i [km] is the length of region i , and l_i [km] is the average trip length of a vehicle in the same region. Moreover, v_i^f [km/h] is the free-flow speed of region i given by

$$v_i^f = q_i^C (\rho_i^C)^{-1}, i \in \mathcal{N}, \quad (5)$$

where q_i^C [veh/h] is the capacity flow² of region i . The backward congestion propagation speed v_i^C [km/h], and the constant b_i^C [veh/h], for region i are defined in a manner that ensures that the function $g_i(\rho_i)$ is continuous as follows

$$v_i^C = q_i^C (\rho_i^J - \rho_i^C)^{-1}, i \in \mathcal{N}, \quad (6a)$$

$$b_i^C = \rho_i^J q_i^C (\rho_i^J - \rho_i^C)^{-1}, i \in \mathcal{N}. \quad (6b)$$

Flows exiting the network through destination regions and transfer flows between regions are calculated according to the MFDs total inter-regional flow, $g_i(\rho_i(t))$, see (3). Moreover

transfer flows between regions are further limited by their inter-boundary capacity. This is modelled via the inter-boundary region i to region l capacity function, $c_{il} : \mathbb{R}_+ \rightarrow \mathbb{R}_+$, that is given by

$$c_{il}(\rho_l) = \begin{cases} c_{il}^{\max}, & \rho_l \leq \rho_{il}^- \\ r_l(b_l^C - v_l^C \rho_l), & \rho_l > \rho_{il}^- \end{cases}, \quad (7)$$

with $i \in \mathcal{N}, l \in \mathcal{S}_i$, and where $c_{il}^{\max} = r_l(b_l^C - v_l^C \rho_{il}^-) \in \mathbb{R}_+$ is the maximum inter-boundary capacity flow from region i to region l , and $\rho_{il}^- \in \mathbb{R}_+$ is the critical inter-boundary density threshold between region i and region l . The transfer flow from region i to region l , $l \in \mathcal{S}_i$, is given by

$$g_{il}(\rho_i, \rho_l) = \min(w_{il} g_i(\rho_i), c_{il}(\rho_l)), \quad (8)$$

with $i \in \mathcal{N}, l \in \mathcal{S}_i$, and where $w_{il} \in \mathcal{W}_i$ are the region i outflow split constants with the set defined as

$$\mathcal{W}_i = \{w_{il}, c_i \in \mathbb{R}_+ : l \in \mathcal{S}_i, c_i + \sum_{l \in \mathcal{S}_i} w_{il} = 1\}, \forall i \in \mathcal{N}, \quad (9)$$

where $c_i \in \mathcal{W}_i$ in (9) is the rate of vehicles that end their trip in region i . The continuous-time evolution of the vehicle density state of each region i , $\rho_i(t)$, is given by

$$\begin{aligned} \dot{\rho}_i(t) = & \frac{1}{L_i} \left(-c_i g_i(\rho_i(t)) - \sum_{l \in \mathcal{S}_i} g_{il}(\rho_i(t), \rho_l(t)) \right. \\ & \left. + \sum_{j \in \mathcal{P}_i} g_{ji}(\rho_j(t), \rho_i(t)) + u_i(t) \right), \forall i \in \mathcal{N}. \end{aligned} \quad (10)$$

The first term in the right hand side of (10) is the flow exiting the network through destination region i , the second term is the flow towards successor nodes, the third term is the flow from predecessor nodes and the last term, $u_i(t)$ [veh/h], is the serviced demand admitted to the network through the origin region i and it is considered a control variable.

We proceed the analysis under the following assumption:

Assumption 1. For each transfer flow from region i to region j , the following relation holds, $c_{ij}(\rho_j^C) > w_{ij} g_i(\rho_i^C)$.

Remark 1. In the density intervals $\rho_i(t) \in [0, \rho_i^C], \rho_j(t) \in [0, \rho_j^C]$, Assumption 1 results in (8) always yielding inter-regional transfer flows from region i to region j satisfying $g_{ij}(\rho_i(t), \rho_j(t)) = w_{ij} g_i(\rho_i(t))$.

Assumption 1 plays a central role in the subsequent analysis. For conciseness the traffic dynamics are defined in a compact form as follows:

Traffic Model 1. The traffic dynamics of the considered n -region connected traffic network are described by (3), (7), (8), and (10).

¹Internal traffic flow is observed/described in a 1 [Km] road stretch.

²Capacity flow is the maximum flow that can be supported by region i ; it is yielded by the FD at the critical density point, ρ_i^C .

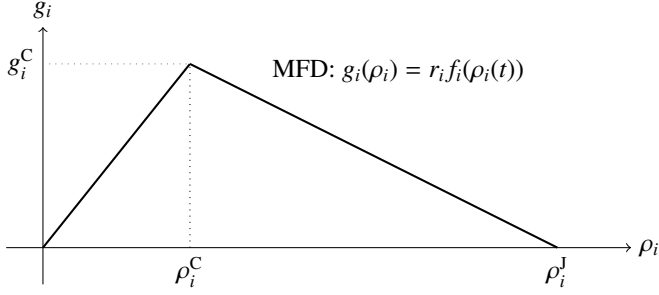


Figure 1: Region i total inter-regional traffic flow $g_i(\rho_i(t))$, approximated by a triangular macroscopic fundamental diagram (MFD).

3. Problem Statement and Optimality Considerations

3.1. Optimization problem

To enable the design of efficient demand management schemes, an optimization problem for demand allocation is formulated yielding *throughput-optimal equilibria*, i.e. a system state characterized by maximum vehicle network throughput or maximum serviced vehicle demand with respect to the network boundaries.

Optimization Problem 1. For an n -region traffic network with traffic dynamics described by Traffic Model 1, solve:

$$\max_{(\rho, \mathbf{u})} \sum_{i \in \mathcal{N}} u_i \quad (11a)$$

$$\text{s.t.} : 0 \leq \rho_i \leq \rho_i^C, \quad i \in \mathcal{N} \quad (11b)$$

$$u_i^{\min} \leq u_i \leq u_i^{\max}, \quad i \in \mathcal{N} \quad (11c)$$

$$\sum_{j \in \mathcal{P}_i} g_{ji}(\rho_j, \rho_i) + u_i - c_i g_i(\rho_i) - \sum_{l \in \mathcal{S}_i} g_{il}(\rho_i, \rho_l) = 0, \quad i \in \mathcal{N} \quad (11d)$$

where $u_i^{\min}, u_i^{\max} \in \mathbb{R}_+$ are selected in a manner that the feasibility of the optimization problem is ensured.

Remark 2. The constraint (11b) stems from practical/physical considerations/observations i.e. an equilibrium point characterized by free-flow conditions is desirable. In (11c) we allow u_i^{\min} to take values that serve the vehicle demand objective. This ensures that demand takes non-negative values, since $u_i \in \mathbb{R}_+, i \in \mathcal{N}$, and enables the formulation of different problems that may either aim to maximize the total throughput or suitably constraint the problem based on some minimum practical value serving realistic regional demand. The justification for u_i^{\max} follows in a similar fashion, noting also that its value in practice may also depend on the structure and parameters of the traffic network.

Remark 3. An issue of feasibility may arise in (11), due to the requirement to simultaneously satisfy (11b) - (11d). One way to overcome this, noting that there is some flexibility in the design of u_i^{\min} and u_i^{\max} , is by obtaining some value of \mathbf{u} satisfying only (11b), and (11d), and then designing u_i^{\min}, u_i^{\max} such that (11c) holds. The obtained feasible values u_i^{\min} and u_i^{\max} can be adapted further to be in compliance with historical data.

3.2. Problem Statement

As already mentioned in Section 1, urban transportation networks frequently suffer from congestion since some regions of the network attract more vehicles than others. Hence this work aims to address the following problem:

Problem 1. For the Traffic Model 1 and under Assumption 1:

1. define an optimal throughput DM solution, based on Optimization Problem 1,
2. design a DM scheme that enables convergence guarantees to free-flow steady state values and is applicable to any (connected) traffic network configuration.

The first condition is associated with the efficiency of DM schemes, aiming to obtain suitable solutions to Optimization Problem 1. The second condition is the main goal of the DM approach, i.e., to ensure that system states attain a desired equilibrium characterised by free-flow conditions, and also that the controller is supplemented by stability guarantees. Additionally, it is required that the DM controller is applicable to any connected traffic network configuration.

3.3. Optimal Solution

Assumption 1 results in inter-regional transfer flows from region i to region j equal to $g_{ij}(\rho_i(t), \rho_j(t)) = w_{ij}g_i(\rho_i(t))$. As a result, the equality constraint (11d) simplifies at steady state conditions to

$$\sum_{j \in \mathcal{P}_i} w_{ji}g_j(\rho_j) + u_i - c_i g_i(\rho_i) - \sum_{l \in \mathcal{S}_i} w_{il}g_i(\rho_i) = 0, \quad i \in \mathcal{N}, \quad (12)$$

and Optimization Problem 1 is given by (11a), (11b), (11c) and (12), and has linear constraints. Moreover, it is also convex and due to advancements in optimization theory and computing, obtaining solutions of convex, linear optimization problems is a relatively easy task serviced by a plethora of commercial solvers that yield solutions in a matter of seconds, even for large-scale problems.

The solution of Optimization Problem 1 with (12) yields optimal equilibria, $(\hat{\rho}, \hat{\mathbf{u}})$, characterized by maximum serviced vehicle demand fulfilling the network inter-boundary demand allocation task.

3.4. Stability Issues

Simulation results (see Figs. 2-5 and the discussion in Section 5) show that operating the system at optimal equilibrium points may result in stability issues. In particular, when an optimal equilibrium point coincides with the local critical density, as is frequently the case, then an arbitrary small increase in density yields substantial deviations in density trajectories, and in many cases leads to gridlock behaviour. As a result, an inherent trade-off between optimality and stability is recognized since when the system operates in a suboptimal way, avoiding equilibrium points at the critical density, then its operation is more robust to disturbances. This offers motivation to rigorously explore the stability properties of the traffic network system.

4. Traffic Network Stability

Motivated by the discussion in the previous section, this section explores the stability properties of traffic networks under constant demand and a proposed proportional feedback demand management scheme.

4.1. Equilibria

Below we provide a definition of the equilibrium points of Traffic Model 1 under interest, to facilitate the analysis later on.

Definition 1. For the Traffic Model 1 under control action $\mathbf{u}^* \in \mathbb{R}_+^n$, an equilibrium point ρ^* , satisfies

$$\left(-c_i g_i(\rho_i^*) - \sum_{l \in \mathcal{S}_i} g_{il}(\rho_i^*, \rho_l^*) + \sum_{j \in \mathcal{P}_i} g_{ji}(\rho_j^*, \rho_i^*) + u_i^* \right) = 0, \forall i \in \mathcal{N}. \quad (13)$$

Next, an investigation is conducted to identify conditions that result in well behaved dynamics such that the solutions of Traffic Model 1 converge to an equilibrium point, ρ^* .

4.2. Stability Analysis under Constant Demand

The behaviour of Traffic Model 1, when its equilibria lie strictly within the free-flow region of operation are investigated next. More explicitly, by means of Lyapunov analysis, sufficient conditions for stability for the Traffic Model 1, are derived.

Theorem 1. Consider the Traffic Model 1, let Assumption 1 hold, let $u_i(t) = u_i^*$, $i \in \mathcal{N}$, and consider an equilibrium point ρ^* , such that $\rho_i^* \in [0, \rho_i^C]$, $\forall i \in \mathcal{N}$. Then, if

$$c_i > \frac{1}{r_i v_i^f} \left(\sum_{j \in \mathcal{P}_i} \frac{a_{ji}}{4} \right), \forall i \in \mathcal{N}, \quad (14a)$$

$$a_{ji} = w_{ji} r_j v_j^f, j \in \mathcal{P}_i, i \in \mathcal{N}, \quad (14b)$$

then, the solutions to Traffic Model 1 locally converge to ρ^* . Moreover, if $u_i^* = \hat{u}_i$, $\forall i \in \mathcal{N}$, where \hat{u}_i is a solution to Optimization Problem 1, then the aforementioned equilibrium point globally solves Optimization Problem 1.

Proof. Let the error state $\mathbf{e}(t) \in \mathbb{R}^n$ be defined as

$$\mathbf{e}(t) = [e_1(t), \dots, e_n(t)]^T, \quad (15a)$$

$$e_i(t) = \rho_i(t) - \rho_i^*. \quad (15b)$$

The following Lyapunov candidate $V : \mathbb{R}^n \rightarrow \mathbb{R}$ is selected

$$V(\mathbf{e}(t)) = \sum_{i \in \mathcal{N}} \frac{L_i}{2} (e_i(t))^2, \quad (16a)$$

$$V(\mathbf{0}) = 0 \text{ and } V(\mathbf{e}(t)) > 0 \text{ in } \mathbb{R}^n \setminus \{\mathbf{0}\}. \quad (16b)$$

Next we consider solutions to Traffic Model 1 within some connected subset $\mathcal{M} \subset \mathbb{R}^n$, that contains the equilibrium point, given by

$$\mathcal{M} = \{\rho : \forall i \in \mathcal{N}, \rho_i^* \in [0, \rho_i^C], V(\rho) \leq \epsilon\}. \quad (17)$$

It is signified that a suitable selection of ϵ , can restrict $\rho_i(t) \in [0, \rho_i^C]$. Moreover, under Assumption 1 the following inequality $c_{ij}(\rho_j(t)) \geq c_{ij}(\rho_j^C) > w_{ij} g_i(\rho_i^C) \geq w_{ij} g_i(\rho_i(t))$ holds $\forall \rho_i(t) \in [0, \rho_i^C]$ and $\forall \rho_j(t) \in [0, \rho_j^C]$, allowing the simplification of (10). Hence, within \mathcal{M} it holds that (8) is always equal to $w_{il} g_i(\rho_i(t))$ which is always valid when Assumption 1 holds (by selecting ϵ). Employing (10), $u_i(t) = u_i^*$, and invoking Assumption 1, the derivative of (16) is given by

$$\dot{V}(t) = \sum_{i \in \mathcal{N}} e_i(t) \left(\sum_{j \in \mathcal{P}_i} w_{ji} r_j f_j(\rho_j(t)) + u_i^* - r_i f_i(\rho_i(t)) \right). \quad (18)$$

At equilibrium, $\dot{\rho}_i = 0$; thus the following holds

$$\frac{1}{L_i} \left(\sum_{j \in \mathcal{P}_i} w_{ji} r_j f_j(\rho_j^*) + u_i^* - r_i f_i(\rho_i^*) \right) = 0. \quad (19)$$

The parenthesis in (19) is subtracted from (18); this yields

$$\dot{V}(t) = \sum_{i \in \mathcal{N}} e_i(t) \left(\sum_{j \in \mathcal{P}_i} w_{ji} r_j (f_j(\rho_j(t)) - f_j(\rho_j^*)) - r_i (f_i(\rho_i(t)) - f_i(\rho_i^*)) \right). \quad (20)$$

For $\rho(t) \in \mathcal{M}$ (20) leads to

$$\dot{V}(t) = \sum_{i \in \mathcal{N}} e_i(t) \left(\sum_{j \in \mathcal{P}_i} w_{ji} r_j v_j^f e_j(t) - r_i v_i^f e_i(t) \right). \quad (21)$$

Expanding (21) via (9) yields

$$\dot{V}(t) = \sum_{i \in \mathcal{N}} e_i(t) \left(\sum_{j \in \mathcal{P}_i} w_{ji} r_j v_j^f e_j(t) - c_i r_i v_i^f e_i(t) - \sum_{l \in \mathcal{S}_i} w_{il} r_i v_i^f e_i(t) \right), \quad (22)$$

where $w_{il}, c_i \in \mathcal{W}_i$ (see (9)). To compact (22) the following constant is defined

$$\gamma_i = c_i r_i v_i^f, i \in \mathcal{N}. \quad (23)$$

Employing the constants from (14b) and (23) in (22) yields

$$\dot{V}(t) = \sum_{i \in \mathcal{N}} \left(\sum_{j \in \mathcal{P}_i} a_{ji} e_i(t) e_j(t) - (\gamma_i + \sum_{l \in \mathcal{S}_i} a_{il}) e_i^2(t) \right). \quad (24)$$

Using the following perfect squares identity

$$\beta xy = \frac{\beta}{4} x^2 + \beta y^2 - \left(\sqrt{\frac{\beta}{4}} x - \sqrt{\beta} y \right)^2 \quad (25)$$

on (24) leads to

$$\begin{aligned} \dot{V}(t) = & \sum_{i \in \mathcal{N}} \sum_{j \in \mathcal{P}_i} \left\{ \frac{a_{ji}}{4} e_i^2(t) + a_{ji} e_j^2(t) - \left(\sqrt{\frac{a_{ji}}{4}} e_i(t) \right. \right. \\ & \left. \left. - \sqrt{a_{ji}} e_j(t) \right)^2 \right\} - \sum_{i \in \mathcal{N}} \left(\gamma_i + \sum_{l \in \mathcal{S}_i} a_{il} \right) e_i^2(t). \end{aligned} \quad (26)$$

Further manipulation of (26) yields

$$\begin{aligned}\dot{V}(t) = & - \sum_{i \in \mathcal{N}} (\gamma_i - \sum_{j \in \mathcal{P}_i} \frac{a_{ji}}{4}) e_i^2(t) \\ & - \sum_{i \in \mathcal{N}} \sum_{j \in \mathcal{P}_i} \left(\sqrt{\frac{a_{ji}}{4}} e_i(t) - \sqrt{a_{ji}} e_j(t) \right)^2.\end{aligned}\quad (27)$$

If (14) holds then (27) is negative definite in $\mathcal{M} \setminus \{\rho^*\}$ and zero at $\rho(t) = \rho^*$, i.e.

$$\dot{V}(\mathbf{e}) \leq - \sum_{i \in \mathcal{N}} \zeta_i e_i^2(t) < 0 \text{ in } \mathcal{M} \setminus \{\mathbf{0}\}, \quad (28a)$$

$$\zeta_i = \gamma_i - \sum_{j \in \mathcal{P}_i} \frac{a_{ji}}{4}, \quad (28b)$$

$$\dot{V}(\mathbf{0}) = 0, \quad (28c)$$

and by [28, Theorem 4.1] it follows that $\mathbf{e} = \mathbf{0}$ is asymptotically stable, which implies that $\lim_{t \rightarrow \infty} \rho_i(t) = \rho_i^*$, $\forall i \in \mathcal{N}$. Moreover, if $\mathbf{u}^* = \hat{\mathbf{u}}$ then by (12) and (13), $\rho^* = \hat{\rho}$, and the aforementioned equilibrium point globally solves/satisfies Optimization Problem 1. \square

The significance of the newly derived criterion, (14), is that it provides locally-verifiable sufficient conditions for stability which enable an assessment of the network stability properties at the presence of some constant demand input. However, since we do not consider the case $\rho_i^* = \rho_i^C$, $i \in \mathcal{N}$, this does not address the issue discussed in Section 3.4, which has been observed at particularly this case. Nevertheless, the presented analysis facilitates the solution to this issue, as demonstrated below.

4.3. Stabilizing Demand Management Scheme

In the last paragraph of Section 3.4, an inherent trade-off between optimality and stability was recognized. In particular, simulations revealed that the system is sensitive to arbitrary small deviations from the optimal/critical equilibrium to the congested region of operation. This unstable behaviour (see Figs. 2-5 and the discussion in Section 5), motivates the development of a stabilizing controller that enables stability guarantees even at the congested region of operation. We propose a controller described by

$$u_i(t) = [\bar{u}_i - k_{p_i} \rho_i(t)]_0^{u_i^{\max}}, \quad i \in \mathcal{N}, \quad (29)$$

where $k_{p_i} \in \mathbb{R}_+ \setminus \{0\}$ and \bar{u}_i is a design constant, that may be selected by taking into account optimality considerations and satisfies the following condition by design

$$0 < \bar{u}_i - k_{p_i} \rho_i^* < \bar{u}_i^{\max}. \quad (30)$$

The selection of the constants \bar{u}_i and k_{p_i} rely on knowledge of the local equilibrium density ρ_i^* , $i \in \mathcal{N}$. When feasible, this value may be provided centrally, through historical data, or by solving Optimization Problem 1. Alternatively, the design could satisfy (30) for a range of local equilibrium values, e.g. for all $\rho_i \in [0, \rho_i^C]$, $i \in \mathcal{N}$.

Theorem 2. Consider Traffic Model 1 under the action of (29), (30), and let Assumption 1 hold. Then, if

$$k_{p_i} > r_i v_i^f + \sum_{j \in \mathcal{P}_i} \frac{\alpha_{ji}}{4} + \sum_{j \in \mathcal{S}_i} \alpha_{ij}, \quad i \in \mathcal{N}, \quad (31a)$$

$$\alpha_{ji} = w_{ji} r_j v_j^L, \quad i \in \mathcal{N}, j \in \mathcal{P}_i, \mathcal{S}_i, \quad (31b)$$

$$v_j^L = \max(v_j^f, v_j^C), \quad j \in \mathcal{N} \quad (31c)$$

then, the solutions of Traffic Model 1 locally converge to an equilibrium point ρ^* . Moreover, if $u_i^* = \hat{u}_i$, $\forall i \in \mathcal{N}$, where \hat{u}_i is a solution to Optimization Problem 1, then the aforementioned equilibrium point globally solves Optimization Problem 1.

Proof. The Lyapunov candidate (16), $V : \mathbb{R}^n \rightarrow \mathbb{R}$, is employed. Here we consider solutions to Traffic Model 1 within a local connected subset $\mathcal{K} \subset \mathbb{R}^n$, where \mathcal{K} is given by

$$\mathcal{K} = \{\rho : \rho_i^* \in [0, \rho_i^C], i \in \mathcal{N}, V(\mathbf{e}) \leq \varepsilon\}. \quad (32)$$

By suitably selecting ε , it can be shown, through Assumption 1, that within \mathcal{K} , (8) is always equal to $w_{ij} g_i(\rho_i(t))$. Moreover, for sufficiently small values of ε , the controller due to (30) does not reach its bounds. Employing (10), (29), and invoking Assumption 1, the derivative of V is

$$\dot{V}(t) = \sum_{i \in \mathcal{N}} e_i(t) \left(\sum_{j \in \mathcal{P}_i} w_{ji} r_j f_j(\rho_j(t)) + \bar{u}_i - k_{p_i} \rho_i(t) - r_i f_i(\rho_i(t)) \right). \quad (33)$$

The parenthesis in (19) is subtracted from (33); this yields

$$\begin{aligned}\dot{V}(t) = & \sum_{i \in \mathcal{N}} e_i(t) \left(\sum_{j \in \mathcal{P}_i} w_{ji} r_j (f_j(\rho_j(t)) - f_j(\rho_j^*)) + \bar{u}_i \right. \\ & \left. - u_i^* - k_{p_i} \rho_i(t) - r_i (f_i(\rho_i(t)) - f_i(\rho_i^*)) \right).\end{aligned}\quad (34)$$

Also due to (30), there exists ε such that $u_i^* = \bar{u}_i - k_{p_i} \rho_i^*$, and (34) simplifies to

$$\begin{aligned}\dot{V}(t) = & \sum_{i \in \mathcal{N}} \left(\sum_{j \in \mathcal{P}_i} w_{ji} r_j e_i(t) (f_j(\rho_j(t)) - f_j(\rho_j^*)) \right. \\ & \left. - k_{p_i} e_i^2(t) - r_i e_i(t) (f_i(\rho_i(t)) - f_i(\rho_i^*)) \right).\end{aligned}\quad (35)$$

By inspecting (3), $f_i(\rho_i(t))$ satisfies the Lipschitz condition globally, with Lipschitz constant v_i^L equal to (31c); hence

$$\forall i \in \mathcal{N}, |f_i(\rho_i(t)) - f_i(\rho_i^*)| \leq v_i^L |\rho_i(t) - \rho_i^*|. \quad (36)$$

Employing (36) in (35) and (31b) yields

$$\dot{V}(t) \leq \sum_{i \in \mathcal{N}} \sum_{j \in \mathcal{P}_i} \alpha_{ji} |e_i(t)| |e_j(t)| - \sum_{i \in \mathcal{N}} (k_{p_i} - r_i v_i^L) e_i^2(t) \quad (37a)$$

$$\begin{aligned}\leq & \sum_{i \in \mathcal{N}} \sum_{j \in \mathcal{P}_i} \left\{ \frac{\alpha_{ji}}{4} e_i^2(t) + \alpha_{ji} e_j^2(t) - \left(\sqrt{\frac{\alpha_{ji}}{4}} |e_i(t)| - \sqrt{\alpha_{ji}} |e_j(t)| \right)^2 \right\} \\ & - \sum_{i \in \mathcal{N}} (k_{p_i} - r_i v_i^L) e_i^2(t),\end{aligned}\quad (37b)$$

where (25) was used to derive (37b). Further manipulation of (37b) yields

$$\begin{aligned} \dot{V}(t) \leq & - \sum_{i \in \mathcal{N}} \sum_{j \in \mathcal{P}_i} \left(\sqrt{\frac{\alpha_{ji}}{4}} |e_i(t)| - \sqrt{\alpha_{ji}} |e_j(t)| \right)^2 \\ & - \sum_{i \in \mathcal{N}} (k_{p_i} - r_i v_i^L - \sum_{j \in \mathcal{P}_i} \frac{\alpha_{ji}}{4} - \sum_{j \in \mathcal{S}_i} \alpha_{ij}) e_i^2(t). \end{aligned} \quad (38)$$

If (31a) holds then (38) is negative definite in $\mathcal{K} \setminus \{\mathbf{0}\}$ and zero at $\rho(t) = \rho^*$, i.e.

$$\dot{V}(\mathbf{e}) \leq - \sum_{i \in \mathcal{N}} \xi_i e_i^2(t) < 0 \text{ in } \mathcal{K} \setminus \{\mathbf{0}\}, \quad (39a)$$

$$\xi_i = k_{p_i} - r_i v_i^L - \sum_{j \in \mathcal{P}_i} \frac{\alpha_{ji}}{4} - \sum_{j \in \mathcal{S}_i} \alpha_{ij}, \quad (39b)$$

$$\dot{V}(\mathbf{0}) = 0, \quad (39c)$$

and by [28, Theorem 4.1], $\mathbf{e} = \mathbf{0}$ is asymptotically stable; $\mathbf{e} = \mathbf{0}$ implies that $\lim_{t \rightarrow \infty} \rho(t) = \rho^*$, see (15).

Moreover, if $u_i^* = \hat{u}_i = \bar{u}_i - k_{p_i} \rho_i^*$, $\forall i \in \mathcal{N}$ with $\rho^* = \hat{\rho}$ then by (12) and (13), the solutions of the system under the action of (29), (30), converge to $\hat{\rho}$, achieving a steady state condition that globally satisfies Optimization Problem 1. \square

Theorem 2 yields a stabilizing controller and a sufficient condition for gain selection, i.e. (31a), that recovers system stability even at the congested region of operation. In addition, when the controller coincides with the solution to Optimization Problem 1, then the equilibrium point enables a globally optimal throughput behaviour. Moreover, the proposed analysis is applicable to any network configuration. Hence, all objectives of Problem 1 are met.

Remark 4. The proposed control scheme utilizes the local density, obtained through local measurements, and a centrally provided set point. The latter is obtained by considering the MFD characteristics of the network and optimality considerations, in accordance to optimization problem (11), and using knowledge of the system steady-state behaviour. The MFD characteristics can be obtained by correct network partitioning [29] and proper measurements [26, 30]. Suitable bounds on the demand values may be obtained using practical considerations, associated with each region's capability to admit the demand, and historical data. The optimum-throughput reference states are then communicated to the DM controllers where each controller, utilizing local density measurements, yields an admitted demand decision that is converted into action by suitable means, such as controlling the traffic lights at the network boundaries and/or through route reservation as detailed in [19, 31]. It is noted that several infrastructure-based and infrastructure-free density estimation methods can be employed for local density measurements as detailed in [32, 33].

Next, we validate the analytic results presented in this paper with numerical simulations.

5. Numerical Results

To illustrate the developments of this work and without loss of generality a representative simulation of a 3-region traffic network is conducted aiming to showcase three important points: a) the stable network behaviour under constant control action, illustrating the validity of Theorem 1, b) the unstable network behaviour when a small deviation from the optimal/critical equilibrium occurs to the congested region of operation, and c) the corrective action of the developed control law, (29), steering the network states back to the optimal/critical equilibrium.

Two simulation cases are considered; the first case uses a constant control action close to the optimal control value, $u_i(t) = \hat{u}_i - 0.1, i \in \mathcal{N}$ (see Table 2 for \hat{u}_i), where \hat{u}_i is the solution to Optimization Problem 1 for region i , to be referred to as benchmark network (black dashed line). The second case employs the derived control law (29) (solid blue line); where $\bar{u}_i = \hat{u}_i + k_{p_i} \rho_i^*, i \in \mathcal{N}$ (see Table 2 for the values of $\hat{u}_i, \rho_i^*, k_{p_i}$).

Network parameters are given in Table 1. It is signified that the rates that vehicles end their trip in region i , determined by the parameter $c_i \in \mathcal{W}_i$, satisfy the conditions of Theorem 1 and the gain values k_{p_i} were selected to satisfy the gain selection condition (31a) of Theorem 2. An 80 [min] simulation scenario is conducted. At $t = 30$ [min] and approximately for 1 [min] a small deviation from the optimal/critical equilibrium is introduced in each network in the form of $u_1(t) = u_1(t) + 0.1\hat{u}_1$.

In Figs. 2-5, the green-shaded interval corresponds to the interval before the appearance of the control input deviation, see Fig. 2 $t \in [0, 30]$ [min]. In both cases the density state at each region achieves steady state, see Fig. 3, demonstrating the validity of Theorem 1. However state convergence is slower in the benchmark network (see dashed lines in Fig. 3). This is expected since it lacks the proportional-term operating on the alternative case that speeds up convergence (see solid lines in Fig. 3). At the same interval both networks operate in free-flow conditions, see Fig. 4. The second case, employing $\bar{u}_i = \hat{u}_i + k_{p_i} \rho_i^*, i \in \mathcal{N}$, operates at maximum inter-regional flow, see Fig. 5, in accordance with Optimization Problem 1.

At $t = 30$ [min] a deviation from steady state appears in both networks in the form of $u_1(t) = u_1(t) + 0.1\hat{u}_1$ (beginning of the red-shaded interval) lasting about 1 [min] (see Fig. 2, first row). For the benchmark network (dashed lines), this deviation results in density drop for regions-2,3 and in region-1 getting congested as its density veers from the optimal-throughput equilibrium and attains gridlock status³, i.e., $\rho_1(t) = \rho_1^1$, see Fig. 3. The convergence to a sub-optimal equilibrium is evident as the speed of region-1 decreased to zero, as demonstrated in Fig. 4. Also, inter-regional flow decreased considerably for regions 2 and 3, as depicted in Fig. 5.

An inherent trade-off between optimality and stability is recognized, in the sense that a traffic coordinator can select a sub-optimal control action $u_i(t) = \mu \hat{u}_i, \mu \in (0, 1)$ (thus operating in sub-optimal throughput conditions) to ensure stability, i.e.,

³Gridlock is a condition where a region cannot admit any more vehicles and congestion is so bad that all vehicles come to standstill.

Table 1: 3-region network parameters.

Region 1	Region 2	Region 3
$L_1 = 1.2$	$L_2 = 1$	$L_3 = 0.85$
$l_1 = 0.6$	$l_2 = 0.45$	$l_3 = 0.35$
$v_1^f = 30$	$v_2^f = 35$	$v_3^f = 32$
$\rho_1^f = 118$	$\rho_2^f = 125$	$\rho_3^f = 98$
$\rho_1^c = 26.3$	$\rho_2^c = 28.2$	$\rho_3^c = 24.4$
$c_1 = 0.25$	$c_2 = 0.35$	$c_3 = 0.2$
$w_{21} = 0.5, w_{31} = 0.25$	$w_{12} = 0.15, w_{32} = 0.5$	$w_{13} = 0.1, w_{23} = 0.7$

Table 2: Throughput-optimal equilibria and control gain values k_{p_i} , for the 3-region network with parameters given in Table 1.

Region 1	Region 2	Region 3
$\hat{\rho}_1 = 26.3$	$\hat{\rho}_2 = 28.2$	$\hat{\rho}_3 = 24.4$
$\hat{u}_1 = 620.71$	$\hat{u}_2 = 76.97$	$\hat{u}_3 = 405.06$
$k_{p_1} = 109.86$	$k_{p_2} = 149.5$	$k_{p_3} = 153.4$

that system uncertainty and disturbances are unable to steer the system to congestion.

In contrast to the above, the network employing the control law with the proportional term, described by (29), is not affected by the deviation (solid lines) and the states remain to the optimal-throughput equilibrium in all regions, as shown in Fig. 3. Only a very minor drop in the speed of region-1 (for a very short time) is observed at $t = 30$ [min], see first row in Fig. 4. A minor increase in the admitted demand in region-2 (for a very short time) is also observed. This is attributed to the corrective action of the proportional term (solid lines, Fig. 2, second row). The network operates in free-flow conditions, see Fig. 4, and at maximum inter-regional flow Fig. 5. Hence, the effectiveness of the control law is clearly demonstrated.

In conclusion, the simulation results clearly demonstrate the validity of the results presented in Section 3 and Section 4.

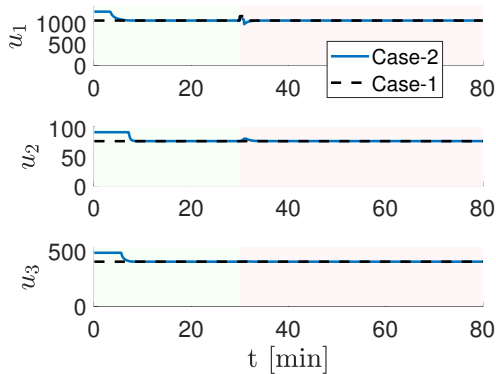


Figure 2: Admitted demand [veh/h]. Case-1 operates at constant demand except for a 1 [min] variation at $t = 30$ [min]. Case-2 demand levels saturate (see $t \in [0, 10]$ [min]) due to the proportional term. Due to demand variation at $t = 30$ [min], stabilizing adjustments are observed for Case-2.

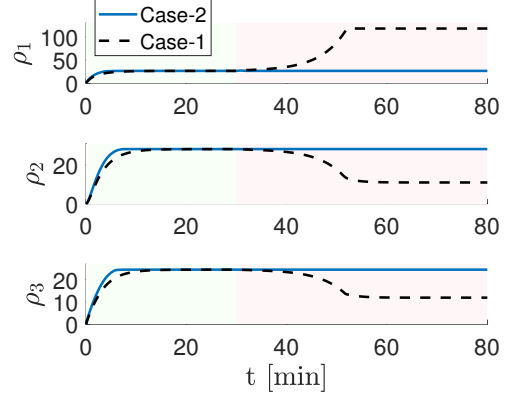


Figure 3: Network density [veh/km]. Initially, both cases achieve steady state. A demand variation at $t = 30$ [min] results in instability for Case-1. Case-2 is stable due to the derived control law.

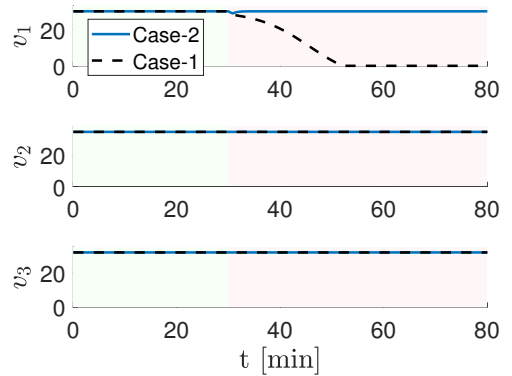


Figure 4: Network speed [km/h]. Initially, vehicles travel at free-flow speed. Due to a demand variation at $t = 30$ [min] region-1 (Case-1) gets congested and eventually attains gridlock status.

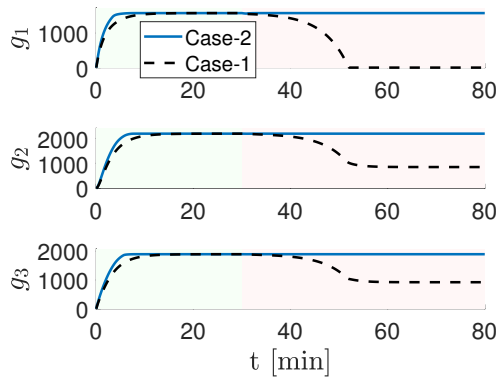


Figure 5: Inter-regional outflow [veh/h]. For the first 30 minutes, both cases achieve similar steady outflow. A demand variation ($t = 30$ [min]) results in instability for Case-1 leading to zero outflow for region-1 and reduced outflow for regions-2,3. Case-2 returns to throughput-optimal operation.

6. Conclusions

This work considered the stability and optimality properties of traffic demand management schemes in traffic networks. First, a suitable optimization problem was formulated that aimed to obtain demand input values that maximize the throughput within traffic networks adhering to regional traffic dynamics with triangular macroscopic fundamental diagrams. A trade-off between stability and optimality was revealed by showing that optimal solutions to this problem may lead to unstable behaviour. To address this issue, we analytically studied the stability properties of traffic networks at the presence of constant demand input and provided suitable local conditions that guarantee stability when the system's equilibrium densities are strictly within the free-flow region, but not at the critical density. However, the critical density case is significant, since the maximum throughput behaviour frequently coincides with the local critical density. To resolve this issue, we proposed a decentralized proportional demand control scheme and suitable local design conditions such that stability is guaranteed. Our analytic results were validated with numerical simulations in a 3-region system that demonstrated the effectiveness and practicality of the presented results.

References

- [1] R. Arnott, K. Small, The economics of traffic congestion, *American scientist* 82 (5) (1994) 446–455.
- [2] M. Papageorgiou, C. Diakaki, V. Dinopoulou, A. Kotsialos, Y. Wang, Review of road traffic control strategies, *Proceedings of the IEEE* 91 (12) (2003) 2043–2067.
- [3] C. F. Daganzo, Urban gridlock: Macroscopic modeling and mitigation approaches, *Transportation Research Part B: Methodological* 41 (1) (2007) 49–62. doi:https://doi.org/10.1016/j.trb.2006.03.001.
- [4] I. I. Sirmatel, N. Geroliminis, Economic model predictive control of large-scale urban road networks via perimeter control and regional route guidance, *IEEE Transactions on Intelligent Transportation Systems* 19 (4) (2018) 1112–1121. doi:10.1109/TITS.2017.2716541.
- [5] A. Kouvelas, M. Saeedmanesh, N. Geroliminis, Enhancing model-based feedback perimeter control with data-driven online adaptive optimization, *Transportation Research Part B: Methodological* 96 (2017) 26–45.
- [6] M. Papageorgiou, Dynamic modeling, assignment, and route guidance in traffic networks, *Transportation Research Part B: Methodological* 24 (6) (1990) 471 – 495. doi:https://doi.org/10.1016/0191-2615(90)90041-V.
- [7] A. Kouvelas, D. Triantafyllos, N. Geroliminis, Hierarchical control design for large-scale urban road traffic networks, in: *Transportation Research Board 97th Annual Meeting*, January 7–11, 2018, Washington, D.C., 2018.
- [8] E. Camacho, C. B. Alba, *Model predictive control*, Springer Science & Business Media, 2013.
- [9] N. Geroliminis, J. Haddad, M. Ramezani, Optimal perimeter control for two urban regions with macroscopic fundamental diagrams: A model predictive approach, *IEEE Transactions on Intelligent Transportation Systems* 14 (1) (2013) 348–359. doi:10.1109/TITS.2012.2216877.
- [10] Z. Zhou, B. De Schutter, S. Lin, Y. Xi, Two-level hierarchical model-based predictive control for large-scale urban traffic networks, *IEEE Transactions on Control Systems Technology* 25 (2) (2017) 496–508. doi:10.1109/TCST.2016.2572169.
- [11] H. Fu, N. Liu, G. Hu, Hierarchical perimeter control with guaranteed stability for dynamically coupled heterogeneous urban traffic, *Transportation Research Part C: Emerging Technologies* 83 (2017) 18–38. doi:https://doi.org/10.1016/j.trc.2017.07.007.
- [12] O. Boufous, C. Roncoli, T. Charalambous, Centralized and distributed multi-region traffic flow control, in: *2020 European Control Conference (ECC)*, 2020, pp. 420–427. doi:10.23919/ECC51009.2020.9143671.
- [13] I. I. Sirmatel, N. Geroliminis, Stabilization of city-scale road traffic networks via macroscopic fundamental diagram-based model predictive perimeter control, *Control Engineering Practice* 109 (2021) 104750. doi:https://doi.org/10.1016/j.conengprac.2021.104750.
- [14] C. Menelaou, S. Timotheou, P. Kolios, C. G. Panayiotou, Joint route guidance and demand management for real-time control of multi-regional traffic networks, *IEEE Transactions on Intelligent Transportation Systems* 23 (7) (2022) 8302–8315. doi:10.1109/TITS.2021.3077870.
- [15] C. Menelaou, S. Timotheou, P. Kolios, C. G. Panayiotou, Convexification approaches for regional route guidance and demand management with generalized mfd, *Transportation Research Part C: Emerging Technologies* 154 (2023) 104245. doi:https://doi.org/10.1016/j.trc.2023.104245.
- [16] J. Haddad, N. Geroliminis, On the stability of traffic perimeter control in two-region urban cities, *Transportation Research Part B: Methodological* 46 (9) (2012) 1159–1176. doi:https://doi.org/10.1016/j.trb.2012.04.004.
- [17] J. Haddad, A. Shraiber, Robust perimeter control design for an urban region, *Transportation Research Part B: Methodological* 68 (2014) 315–332. doi:https://doi.org/10.1016/j.trb.2014.06.010.
- [18] A. Kouvelas, M. Saeedmanesh, N. Geroliminis, Enhancing model-based feedback perimeter control with data-driven online adaptive optimization, *Transportation Research Part B: Methodological* 96 (2017) 26–45. doi:https://doi.org/10.1016/j.trb.2016.10.011.
- [19] C. Menelaou, P. Kolios, S. Timotheou, C. Panayiotou, M. Polycarpou, Controlling road congestion via a low-complexity route reservation approach, *Transportation Research Part C: Emerging Technologies* 81 (2017) 118–136. doi:https://doi.org/10.1016/j.trc.2017.05.005.
- [20] T. Lei, Z. Hou, Y. Ren, Data-driven model free adaptive perimeter control for multi-region urban traffic networks with route choice, *IEEE Transactions on Intelligent Transportation Systems* 21 (7) (2020) 2894–2905. doi:10.1109/TITS.2019.2921381.
- [21] Y. Ning, L. Du, Robust and resilient equilibrium routing mechanism for traffic congestion mitigation built upon correlated equilibrium and distributed optimization, *Transportation Research Part B: Methodological* 168 (2023) 170–205. doi:https://doi.org/10.1016/j.trb.2022.12.006.
- [22] J. Macfarlane, When apps rule the road: The proliferation of navigation apps is causing traffic chaos. it's time to restore order, *IEEE Spectrum* 56 (10) (2019) 22–27.
- [23] J. R. Correa, A. S. Schulz, N. E. Stier-Moses, Selfish routing in capacitated networks, *Mathematics of Operations Research* 29 (4) (2004) 961–976.
- [24] K. Luten, Mitigating Traffic Congestion: The role of demand-side strategies, Tech. rep., U.S. Department of Transport, Federal Highway Administration (10 2004).
- [25] W. Saleh, G. Sammer, Travel demand management and road user pricing: success, failure and feasibility, in: *Travel Demand Management and Road User Pricing*, Routledge, 2016, pp. 1–9.
- [26] N. Geroliminis, C. F. Daganzo, Existence of urban-scale macroscopic fundamental diagrams: Some experimental findings, *Transportation Research Part B: Methodological* 42 (9) (2008) 759–770. doi:https://doi.org/10.1016/j.trb.2008.02.002.

- [27] V. L. Knoop, H. van Lint, S. P. Hoogendoorn, Traffic dynamics: Its impact on the macroscopic fundamental diagram, *Physica A: Statistical Mechanics and its Applications* 438 (2015) 236–250. doi:<https://doi.org/10.1016/j.physa.2015.06.016>.
- [28] H. K. Khalil, *Nonlinear Systems*, 3rd Edition, Pearson Education Limited, 2002.
- [29] M. Saeedmanesh, N. Geroliminis, Dynamic clustering and propagation of congestion in heterogeneously congested urban traffic networks, *Transportation Research Procedia* 23 (2017) 962–979, papers Selected for the 22nd International Symposium on Transportation and Traffic Theory Chicago, Illinois, USA, 24-26 July, 2017. doi:<https://doi.org/10.1016/j.trpro.2017.05.053>.
- [30] D. Helbing, Derivation of a fundamental diagram for urban traffic flow, *The European Physical Journal B* 70 (2009) 229–241.
- [31] C. Makridis, C. Menelaou, S. Timotheou, C. Panayiotou, An implementation of a route reservation architecture, *IFAC-PapersOnLine* 54 (2) (2021) 1–6, 16th IFAC Symposium on Control in Transportation Systems CTS 2021. doi:<https://doi.org/10.1016/j.ifacol.2021.06.042>.
- [32] T. Darwish, K. Abu Bakar, Traffic density estimation in vehicular ad hoc networks: A review, *Ad Hoc Networks* 24 (2015) 337–351. doi:<https://doi.org/10.1016/j.adhoc.2014.09.007>.
- [33] A.-S. A. Al-Sobky, R. M. Mousa, Traffic density determination and its applications using smartphone, *Alexandria Engineering Journal* 55 (1) (2016) 513–523. doi:<https://doi.org/10.1016/j.aej.2015.12.010>.